J. Iron Steel Res. Int. (2020) 27:310–318
https://doi.org/10.1007/s42243-019-00360-5

ORIGINAL PAPER

Optimization of iron and aluminum recovery in bauxite

Qian Long[1,2] · Jun-qi Li[1,2] · Chao-yi Chen[1,2] · Yuan-pei Lan[1,2] · Guo-ling Wei[1,2]

Received: 29 September 2018 / Revised: 25 June 2019 / Accepted: 25 June 2019 / Published online: 20 February 2020
© China Iron and Steel Research Institute Group 2020

Abstract
Recovering iron and aluminum efficiently is the key route to utilize low-grade high-iron bauxite. Aiming to optimize the iron separating process and elevate both Fe and Al recovery ratio, three different Fe–Al recovery processes with different magnetic roasting (R), Bayer leaching process (L) and magnetic separation (S) orders were investigated. The studied processes include bauxite leaching → red mud roasting → magnetic separation (L–R–S), bauxite roasting → magnetic separation → leaching (R–S–L) and bauxite roasting → leaching → magnetic separation (R–L–S). The iron recovery ratio, Fe_2O_3 content in iron concentration and the bauxite dissolution ratio of each process were investigated. Moreover, the optimizations of the leaching, roasting and magnetic separation conditions were studied. Results indicate that the R–S–L process should be an advisable order to recover both alumina and iron. In the three processes, the R–S–L route had the highest alumina dissolution ratio and iron recovery ratio, which was 86.20% and 69.58%, respectively, while the Fe_2O_3 content of the iron concentrate was 40.66%.

Keywords High-iron bauxite · Magnetic roasting · Magnetic separation · Recovery ratio · Dissolution ratio

1 Introduction

Utilization of low-grade bauxite for alumina production has become a worldwide urgent issue due to the increasing aluminum demand and the lack of high-quality bauxite ores [1]. Low-grade bauxite usually contains high iron, high sulfur or high silicon minerals [2–4]. Typically, in low-grade high-iron bauxite, the main ferrous phases are α-FeOOH or hematite (Fe_2O_3) [5]. Separating and recovering iron will contribute to the reduction of red mud (bauxite leaching residue), and the recovered iron concentrate will be provided as a raw material for ironmaking [6, 7]. Besides the separated iron, the alumina minerals in bauxite can be used in alumina production. Thus, numerous studies focused on Fe and Al utilization from high-iron bauxite, and it is believed that magnetic separation and Bayer dissolution is one of the most convenient techniques [8–11].

Magnetic separation is an efficient process to recover iron from ores, but the main ferrous phases in bauxite are goethite or hematite [12], and therefore, the magnetic roasting becomes an indispensable process before magnetic separation which aims to reduce ferrous oxide to magnetite [13]. Moreover, magnetic roasting is not only beneficial for iron recovery, but also valuable to other elements recycling [14]. H_2, CO and coal are the common reducing agents [15, 16] for magnetic roasting; for example, Khaki et al. [17] directly reduced the low-grade iron with coal and then recovered iron by magnetic separation, while Man and Feng [18] tried to reduce iron ore pellets by hydrogen. Zhang et al. [19] proposed a high-temperature reducing and smelting process to recover iron and calcium aluminate slag from high-iron bauxite. On the other hand, many researchers paid attention to iron recovery from red mud by magnetic separation. Li et al. [20] extracted alumina by Bayer process, followed by iron recovery from red mud via a magnetic separation process. Zhu et al. [21] recovered iron from high-iron red mud by a reduction roasting process with adding sodium salt, while Samouhos et al. [22] used hydrogen as a reducing agent to recover iron from red mud between 300 and 480 °C. Utilization of iron from bauxite can be summarized as two methods: (1) recover iron from bauxite ores and (2) separate iron from red mud, but few studies are found to evaluate both iron and alumina utilization by these two methods.

✉ Jun-qi Li
jqli@gzu.edu.cn

[1] Department of Metallurgical Engineering, College of Materials and Metallurgy, Guizhou University, Guiyang 550025, Guizhou, China

[2] Guizhou Province Key Laboratory of Metallurgical Engineering and Process Energy Saving, Guiyang 550025, Guizhou, China

Besides, iron minerals have been reported to make effects on aluminum dissolution in Bayer process [10, 23, 24]. Li et al. [23] found that the conversion of hematite to magnetite in Bayer digestion showed an effect on the dissociation of iron and silicate minerals. Basu [25] reported that the transformation of α-FeOOH to α-Fe_2O_3 at high temperatures results in an improving settling properties. Moreover, it was reported that ferrous sulfate could improve the digestion of diasporic bauxite in the Bayer process [26]. Thus, different forms of iron minerals will affect the alumina dissolution properties in Bayer process; adopting the magnetic roasting process before or after the Bayer process will affect the iron and alumina recovery, because most of the hematite transfers to magnetite, and it was reported that the magnetite may affect alumina dissolution properties [27, 28]. Moreover, when roasting the bauxite before Bayer process, separating iron before or after Bayer process may also affect the iron recovery and alumina dissolution properties. However, few researchers compared the advantages and disadvantages of the Fe and Al recovery ratio of the described routes, causing a scientific and technical confusion for Al–Fe recovery from high-iron bauxite.

Therefore, this investigation aimed to evaluate the optimum process for Fe and Al recovery, and optimize the Fe and Al recovery ratio from bauxite by magnetic roasting, separation and Bayer leaching. Three processes with different treating orders which include the L–R–S [leaching of bauxite (L) → magnetic roasting of red mud (R) → magnetic separation of the roasted red mud (S)], R–S–L (magnetic roasting of bauxite → magnetic separation of roasted bauxite → leaching of separated bauxite) and R–L–S (magnetic roasting of bauxite → leaching of roasted bauxite → magnetic separation of bauxite residue) processes were considered in this work. Meanwhile, different roasting and dissolution conditions were studied, and the iron and aluminum recovery ratios were investigated and discussed.

2 Experimental procedure

2.1 Materials

Pingguo high-iron bauxite (Guangxi, China) was used as the bauxite sample in this work. The bauxite with a particle size of 74 μm (85%) was air-dried. Its chemical components are listed in Table 1, and the main phases are shown in Fig. 1 by X-ray diffraction (XRD) analysis. It can be found that the alumina/silica ratio (A/S) of this bauxite ore is 5.64% and the iron content (Fe_2O_3) is 18.70 wt.%; the main phases are diaspore, goethite, pyrophyllite and perovskite.

Table 1 Main chemical component of studied bauxite

Al_2O_3/wt.%	TFe/wt.%	SiO_2/wt.%	TiO_2/wt.%	A/S
55.80	18.70	9.90	2.81	5.64

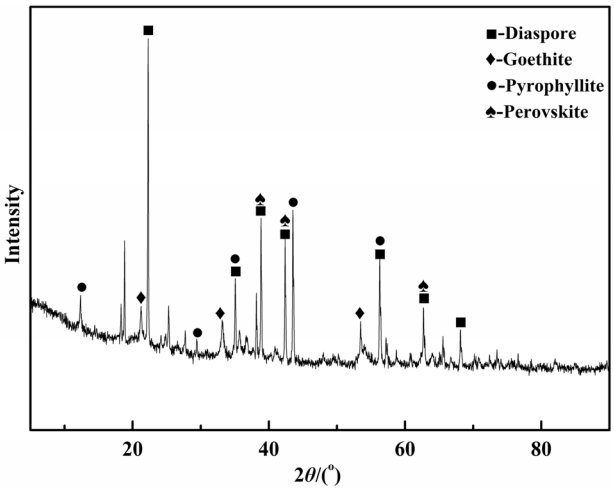

Fig. 1 XRD pattern of high-iron bauxite ore

The circulation liquid and lime (75% active CaO) for Bayer leaching were obtained from Guizhou, China.

2.2 Methods

Three different Al–Fe recovery processes can be found in Fig. 2. As shown in Fig. 2, the L–R–S process means that the bauxite is firstly subjected to Bayer leaching, followed by magnetic roasting of red mud, and then, the roasted red mud would be magnetically separated for iron recovery. The R–S–L process intends to directly magnetize the original bauxite ore by hydrogen roasting and then perform a magnetic separation process, and finally, the treated ores were

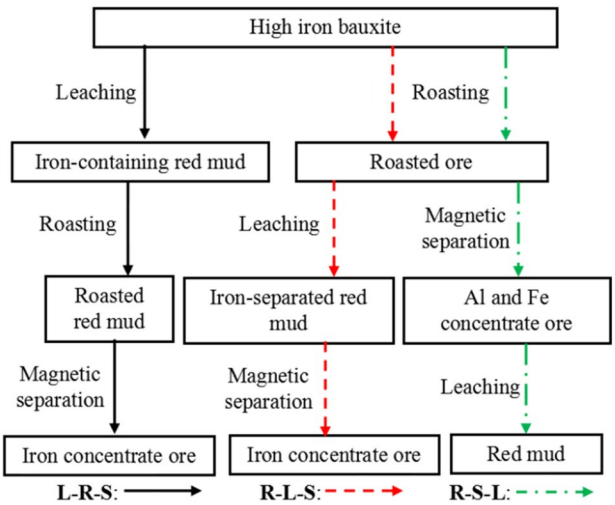

Fig. 2 Schematic of different Al–Fe recovery processes

dissolved into a Bayer process. The R–L–S process has a roasting treatment firstly which is similar with the R–S–L process; however, the roasted ore is subjected to a leaching process, followed by the magnetic separation of red mud.

A high-temperature vacuum atmosphere tube furnace (CVD(G)-09/60/1 Hefei Rixin High Temperature Technology Co., Ltd., China) was used to roast samples in a hydrogen atmosphere with nitrogen as the shielding gas. Moreover, the red mud was firstly dried in a drying oven (202-ABS Shanghai Zhuo Instrument Co., Ltd., China) before other treatments. A magnetic separator (XCGS type Φ50 Shicheng Oasis Mineral Processing Equipment Manufacturing Co., Ltd., China) was used to separate iron and other elements, while the Bayer leaching experiments were done in a steel autoclave (ZWYYL120-06 Weihai Zhengwei Machinery Factory, China).

In the leaching process, various leaching temperatures and time, lime addition amounts and Na_2O concentrations were studied, and the alumina dissolution ratio and the iron content in the red mud were also investigated to determine the better dissolution conditions. Typically, a certain amount of bauxite powder and lime were mixed with a desired volume of circulation liquid in a clean steel autoclave, and then, the steel autoclave was placed in a furnace which was heated in a molten salt media at a desired temperature. After heating, the solution would be subjected to filtration and obtain red mud, and then, the red mud was dried at 100 °C for 25 h. After that, the Al_2O_3, SiO_2 and Fe_2O_3 contents in red mud were measured by chemical analysis. The alumina dissolution ratio can be calculated by following equation:

$$\eta_A = \frac{(A/S)_O - (A/S)_R}{(A/S)_O} \times 100\% \quad (1)$$

where η_A is the actual Al_2O_3 dissolution ratio, %; $(A/S)_O$ is the alumina to silica ratio of bauxite ore; and $(A/S)_R$ is the alumina to silica ratio of red mud.

The Fe_2O_3 content can be calculated by Eq. (2):

$$w_{Fe_2O_3} = \frac{V \times 0.0027925}{0.7m} \times 100\% \quad (2)$$

where $w_{Fe_2O_3}$ is the iron oxide content; V is the volume of potassium dichromate standard solution; and m is the sample mass.

For a magnetic roasting experiment, 45 g dried high-iron bauxite or red mud sample was placed in an alumina boat, and then, the alumina boat was heated in the tube furnace. A 40 mL/min hydrogen flow was used as the reducing gas. In this part, different heating temperatures (300–700 °C) and time (30–90 min) were studied.

In magnetic separation test, 7 g magnetized bauxite or red mud was rushed into the magnetic tube with deionized water and separated for a desired selection time under different magnetic intensities (different working currents, A). After separation, the collected powder was dried in a vacuum drying oven at 80 °C for 12 h, and the iron content of the dried powder was analyzed. The iron recovery ratio can be calculated by following equation:

$$\eta_I = \frac{w_{Fe_2O_3} \times m_C}{w_R \times m_R} \times 100\% \quad (3)$$

where η_I is the iron recovery ratio, %; m_C is the mass of selected iron concentrate, g; m_R is the mass of the roasting ore, g; and w_R is the percentage of Fe_2O_3 in the red mud/original ore after roasting, %.

2.3 Analysis

In all processes, the Al_2O_3 was determined by EDTA complexometric titration method, Fe_2O_3 was measured by the potassium dichromate method, and silica was analyzed by the silicon molybdenum blue colorimetric method. The XRD patterns were recorded by X'Pert PRO MPD (Parnco, Netherlands). The thermogravimetry (TG), derivative thermogravimetry (DTG) and differential thermal analysis (DTA) spectra were tested using a TG/DTG 7300 thermogravimetric differential comprehensive thermal analyzer, and 8.441 mg sample was tested with a heating rate of 10 °C/min at a temperature between 20 and 800 °C in argon.

3 Results and discussion

3.1 Alumina dissolution properties and iron content in red mud

The alumina dissolution properties and iron content in red mud were studied and discussed under different leaching conditions, which included various leaching temperatures and time, lime addition amounts and Na_2O concentrations.

Figure 3 shows the alumina dissolution ratio and the iron content in red mud under various dissolution time. It can be seen that the alumina dissolution ratio increased rapidly when the leaching time increased from 30 to 40 min, and then, the rising rate slowed down. On the other hand, the iron content in red mud was decreased with an increasing dissolution time, which may be due to the ferrous phases dissolving into sodium aluminate solution after a long reaction time [29]. The results in Fig. 3 suggest that the optimization time can be set as 50 min.

The influences of reacting temperature on the alumina dissolution ratio and iron content in red mud are exhibited in Fig. 4. It can be found that the alumina dissolution ratio and iron content in red mud have a similar varied curve with the reacting temperature increasing, where the increasing rate

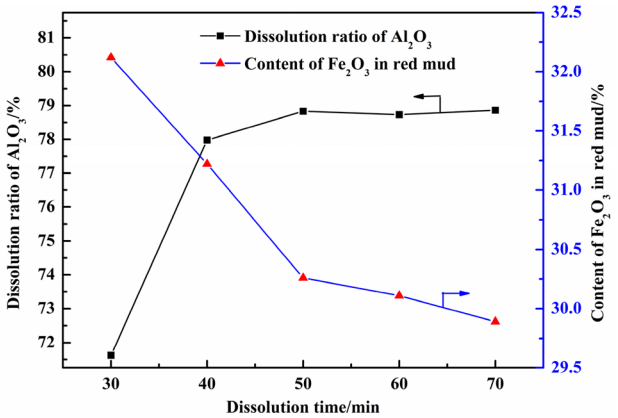

Fig. 3 Dissolution ratio and content of Fe_2O_3 in red mud at different dissolution time under conditions of dissolution temperature of 260 °C, lime addition amount of 6% and Na_2O concentration of 235 g/L

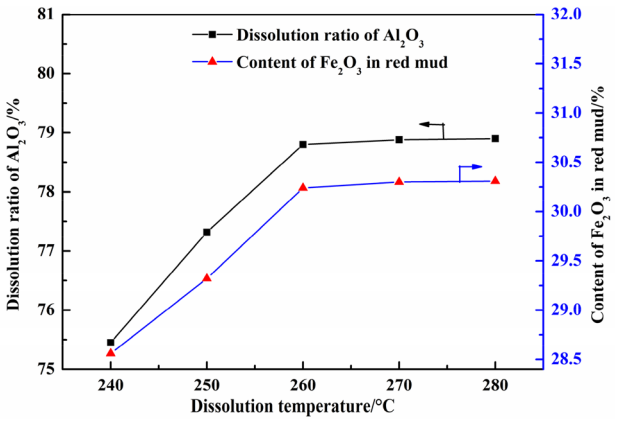

Fig. 4 Dissolution ratio and content of Fe_2O_3 in red mud at different dissolution temperatures under conditions of dissolution time of 50 min, lime addition amount of 6% and Na_2O concentration of 235 g/L

is somewhat constant when the temperature was higher than 260 °C. Therefore, 260 °C can be an expected temperature for alumina leaching.

Figure 5 shows the effects of lime amount on the alumina dissolution ratio and iron content in red mud. It can be found that with 4% lime addition, the iron content in red mud has the highest value. When the lime addition amount increased to 8% or 10%, the iron content in red mud decreased significantly. On the other hand, the Al_2O_3 dissolution ratio increased firstly and then deceased when the lime addition amount increases; when adding 6% lime, the alumina dissolution ratio had the largest value of 79.28%, while the iron content in red mud had a minor decrease. Appropriate amount of lime will react with goethite or diaspore to form calcium hydroxide that will be dehydrated and formed

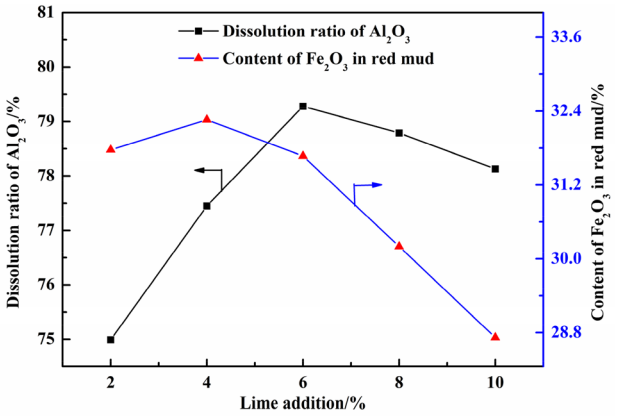

Fig. 5 Dissolution ratio and content of Fe_2O_3 in red mud for different lime additions under conditions of dissolution time of 50 min, dissolution temperature of 260 °C and Na_2O concentration of 235 g/L

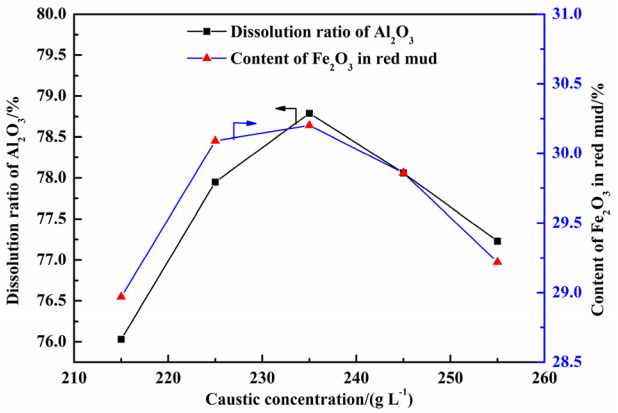

Fig. 6 Dissolution ratio and content of Fe_2O_3 in red mud for different caustic concentrations under conditions of dissolution time of 50 min, dissolution temperature of 260 °C and lime addition amount of 6%

hematite or $Al(OH)_4^-$ later, which is beneficial for the dissolution properties of ores [30], and the related reactions are given as follows:

$$(MOOH)_n + Ca(OH)_2 + H_2O \rightarrow CaM(OH)_3 + (MOOH)_{n-1} + 2OH^- \quad (4)$$

$$CaAl(OH)_3 + 2H_2O \cdot OH^- \rightarrow Al(OH)_4^- + H_2 \quad (5)$$

$$2\left(CaO \cdot Fe(OH)_3\right) \rightarrow 2Ca(OH)_2 + Fe_2O_3 + H_2O \quad (6)$$

where M means Al or Fe. From Fig. 5, it can be concluded that 6% lime addition amount is better.

Figure 6 shows the influence of Na_2O concentration on the leaching properties. It is shown in Fig. 6 that the dissolution ratio and content of Fe_2O_3 in red mud increased firstly and then decreased with an increasing Na_2O concentration. Thus, 235 g/L should be a better Na_2O concentration.

3.2 Effect of magnetic separation conditions on iron recovery

Different conditions of magnetic separation process which include magnetic current (1–4 A), separation time (5–20 min) and cycle times (1–4 times) were investigated to find out an optimum separation condition for iron recovery, and the results are listed in Table 2. As shown in Table 2, with the magnetic current and separation time increasing, the iron recovery ratio increased, but the grade of iron concentrate was found to be decreased. It was reported [31] that a stronger magnetic strength resulted in a lower grade in iron concentrate because the low magnetic minerals were separated together with the expected collections (e.g., Fe_3O_4).

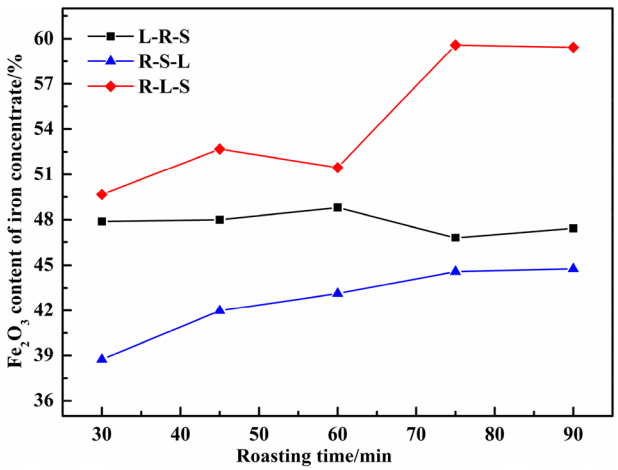

Fig. 7 Fe_2O_3 content in iron concentration with different roasting time in three processes

3.3 Effects of roasting conditions on iron recovery

Different magnetic roasting factors that include the roasting time and temperature were studied here, while the hydrogen flow rate was 40 mL/min. In this part, for leach testing, the reaction time was 50 min, temperature was 260 °C, Na_2O concentration was 235 g/L, and lime addition was 6%. Likewise, an advisable magnetic separation condition was used here according to the above results, where the samples were subjected to 10 min separation under 4 A separation current for one separation cycle.

Figures 7 and 8 show the Fe_2O_3 content in iron concentrate and the iron recovery ratio, respectively, for different roasting time of L–R–S, R–S–L and R–L–S processes.

It can be found from Figs. 7 and 8 that the Fe_2O_3 content of iron concentrate and recovery ratio for L–R–S process were kept at 46.81%–48.00% and 46.36%–48.33%, respectively, which suggests that the roasting time has a little effect on L–R–S route for iron recovery. It may be due to the small particle size of red mud [13] and also revealed that 30 min was enough for the magnetic separation of red mud.

For the R–S–L process, it can be seen from Figs. 7 and 8 that the Fe_2O_3 content of iron concentrates and recovery ratio increase with an increase in roasting time. The recovery ratio of iron was only 44.34% when the roasting time was 30 min, and then, it increased to 64.11% after roasting for 75 min, but further extending the roasting time to 90 min, the recovery ratio had little changes. The Fe_2O_3 content of the iron concentrate of R–S–L process increases after roasting for a longer time, which increased from 38.74% to 44.77% when the roasting time increased from 30 to 90 min.

On the other hand, both the Fe_2O_3 content of iron concentrate and the iron recovery ratio for R–L–S process had the largest value when the bauxite was heated for 75 min, where the Fe_2O_3 content in iron concentrate was 59.59% and the

Table 2 Influences of magnetic separation condition on iron recovery ratio and Fe_2O_3 content in iron concentrate

Magnetic current/A	Separation time/min	Cycle/times	Iron ore concentrate/g	Fe_2O_3 content in iron concentrate/%	Iron recovery/%
1.0	10	1	0.43	51.20	20.92
2.5	10	1	0.61	45.94	26.64
3.5	10	1	0.98	44.49	41.44
4.0	10	1	1.37	43.46	56.59
4.0	5	1	1.12	46.64	49.65
4.0	10	1	1.37	43.46	56.59
4.0	15	1	1.49	40.16	58.89
4.0	20	1	1.64	38.20	59.54
4.0	10	1	1.37	43.46	56.59
4.0	10	2	0.98	48.56	45.20
4.0	10	3	0.82	49.81	38.69
4.0	10	4	0.77	50.17	36.65

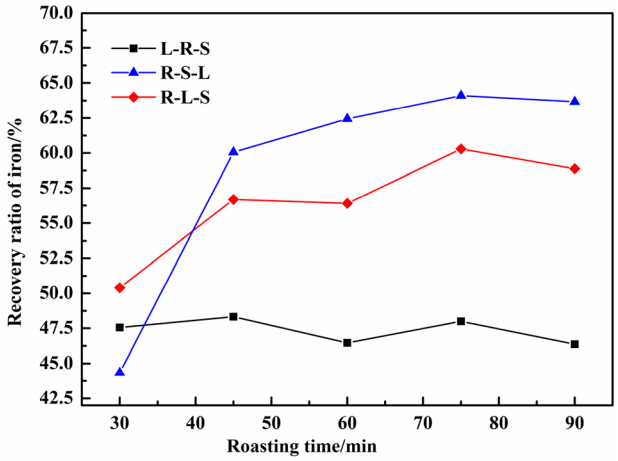

Fig. 8 Iron recovery ratio with different roasting time in three processes

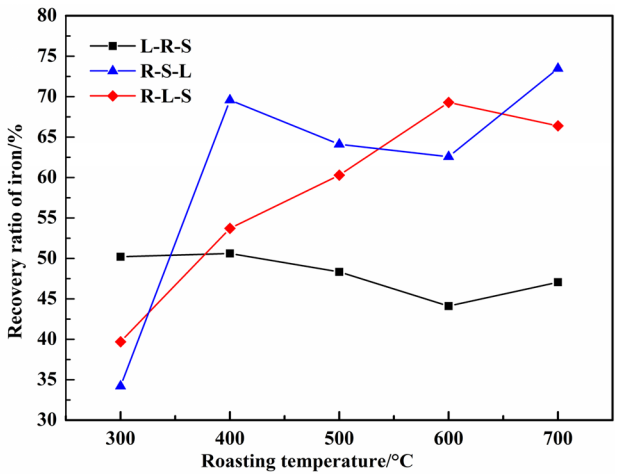

Fig. 10 Recovery ratio of iron with different roasting temperatures in three processes

ratio was found as 60.29%. It is similar to the R–S–L process that with an extending time when the time was shorter than 75 min, both the Fe_2O_3 content and ratio tended to rise. The credible reason should be that longer treating time caused more Fe_2O_3 reduction due to the diffusion. The results in Figs. 7 and 8 indicate that 75 min should be a suitable roasting time.

Figures 9 and 10 show the effects of heating temperature on the Fe_2O_3 content in iron concentrate and recovery ratio, respectively, while the roasting time was 75 min. From Figs. 9 and 10, it can be found that the L–R–S process is not a good choice for recovering iron compared with R–S–L and R–L–S processes. The L–R–S process has a lower iron recovery ratio when the roasting temperature is higher than 400 °C, while the values of Fe_2O_3 content in iron concentrate

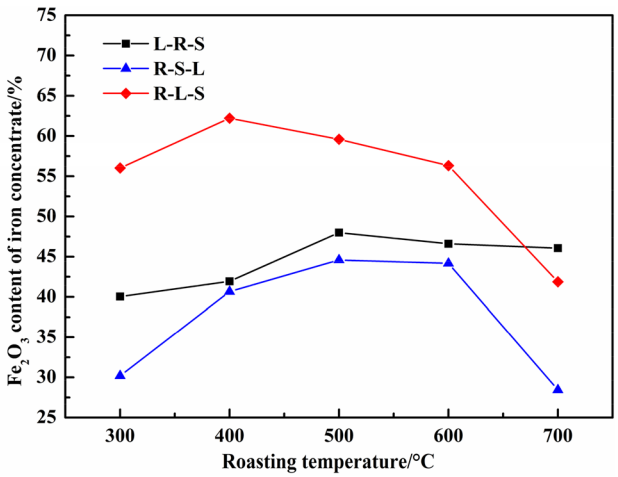

Fig. 9 Fe_2O_3 content in iron concentration with different roasting temperatures in three processes

of L–R–S route are almost between those of R–S–L and R–L–S processes.

Figure 9 shows that the R–L–S process had the largest Fe_2O_3 content of iron concentrate in three routes, and peak value of 62.21% can be found when the roasting temperature was 400 °C, while the highest iron recovery ratio of the R–S–L process was found when the roasting temperature was 600 °C and the recovery ratio was 69.29% (Fig. 10). At a lower heating temperature, the goethite in bauxite cannot be completely removed and the hydrogen gas can hardly react with iron minerals directly due to the decomposition of the crystalline water in ore. With the roasting temperature increasing, more magnetite formed, and owing to the dehydration of the goethite, numerous micropores were generated on the particles which contributed to the reduction process. At 600 °C, the Fe_2O_3 content in iron concentrate of the R–L–S process is found as 56.31%; thus, the roasting temperature for the R–L–S process is better to be set as 600 °C.

Even though the Fe_2O_3 content of iron concentrate for the R–S–L process was lower than that of other two processes (Fig. 9), it can be found from Fig. 10 that the iron recovery ratio was 69.58% and 73.48% when the roasting temperature was 400 and 700 °C, respectively, which was higher than those of the other processes. Therefore, the R–S–L process seems to be a reasonable route to recover more iron by treating every unit bauxite.

3.4 Optimization of iron and alumina recovery

In order to compare these three processes more clearly, the optimization of iron and alumina recovery ratio for each process was summarized and the results are shown in Fig. 11, where the dissolution time was 50 min, the dissolution temperature was 260 °C, lime addition amount was 6%, Na_2O

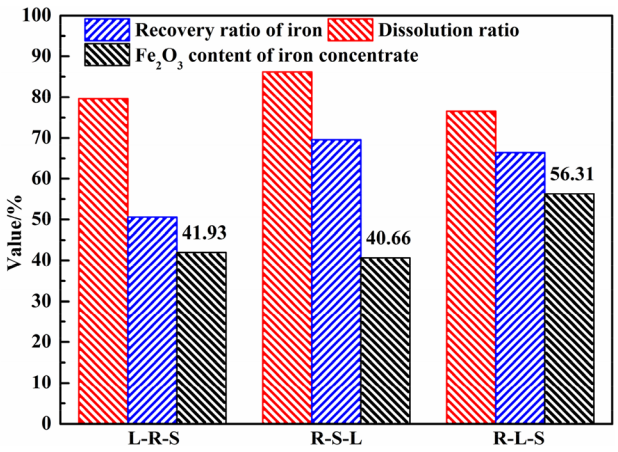

Fig. 11 Dissolution ratio, iron recovery ratio and Fe_2O_3 content in iron concentrate for three processes

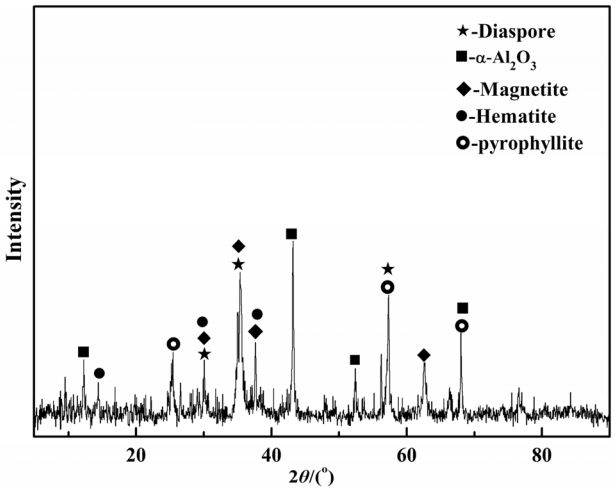

Fig. 12 XRD result of magnetically roasted ore

concentration was 235 g/L, and roasting time was 75 min. The roasting temperature of the R–L–S process was 600 °C, while the roasting temperature of the R–S–L and L–R–S processes was 400 °C.

Figure 11 indicates that in the L–R–S process, the dissolution ratio, iron recovery ratio and Fe_2O_3 content in iron concentrate were 79.60%, 50.61% and 41.93%, respectively. For the R–S–L process, the corresponding characteristic parameters were 86.20%, 69.58% and 40.66%, while in the R–L–S route, they were 76.58%, 69.26% and 56.31%, respectively.

The L–R–S process had a higher dissolution ratio than the R–L–S process, but a lower dissolution ratio than the R–S–L process, while the iron recovery ratio and Fe_2O_3 content in iron concentrate of L–R–S route were lower than those of the other processes. For the R–S–L process, it can be distinguished that the alumina dissolution ratio and iron recovery ratio by this process were higher than those of the L–R–S and R–L–S processes, but the Fe_2O_3 content in iron concentrate was just 40.66%. The iron recovery ratio of the R–L–S process was found as 69.26% and the Fe_2O_3 content in concentrate was 56.31%, which shows that the R–L–S route can be regarded as a better candidate for iron recovery. However, the alumina dissolution ratio of the R–L–S process was 76.58%, which was much lower than that of the R–S–L process.

Thus, it can be concluded from Fig. 11 that the R–S–L process is a suitable process for both alumina and iron recovery, where it has the largest dissolution ratio and iron recovery ratio. However, in this process, the magnetic separation is earlier than the leaching process, and part of alumina is inevitably separated into the iron concentrate which cannot be utilized in the Bayer process. In current investigations, we found that under the optimum conditions of the R–S–L route, 32.80%–65.17% of alumina in bauxite went into iron concentrate. Thus, further special studies need to be focused on the reduction in the alumina loss during the separation process. Moreover, the Fe_2O_3 content in iron concentrate needs to be elevated for further industrial applications of the iron concentrate.

3.5 Mechanism of magnetic roasting

Figure 12 shows the XRD pattern of the sample roasted at 400 °C for 75 min in a 40 mL/min hydrogen flow.

Compared with the XRD pattern of un-roasted bauxite in Fig. 1, it can be seen from Fig. 12 that the ore roasted at 400 °C contains diaspore, α-Al_2O_3, magnetite, hematite and pyrophyllite, which indicates that all goethite has been transformed to magnetite and hematite.

Aiming to reveal the mechanism of the magnetic roasting process, one raw ore sample was subjected to TG/DTG analysis and the results are shown in Fig. 13.

Figures 13 shows that the total mass loss during the heating process was 12.85%, which can be divided into four parts including: (1) at 20–200 °C, the mass loss was 0.62%, owing to the vaporization of free water; (2) at 200–400 °C, the mass loss at 345 °C reached 2.2% because of the decomposition of the diaspore, and at 345–400 °C, the mass kept somewhat invariant; (3) at 400–600 °C, the mass loss was further increased to 9.56%; and (4) at 600–800 °C, the mass decreased slowly, and the mass loss was 0.47%.

According to the XRD (Figs. 1 and 12) and TG/DTG results, the reactions during the magnetic roasting process can be summarized as follows:

$$2\alpha\text{ - AlOOH} \rightarrow \alpha\text{ - } Al_2O_3(s) + H_2O(g) \quad (7)$$

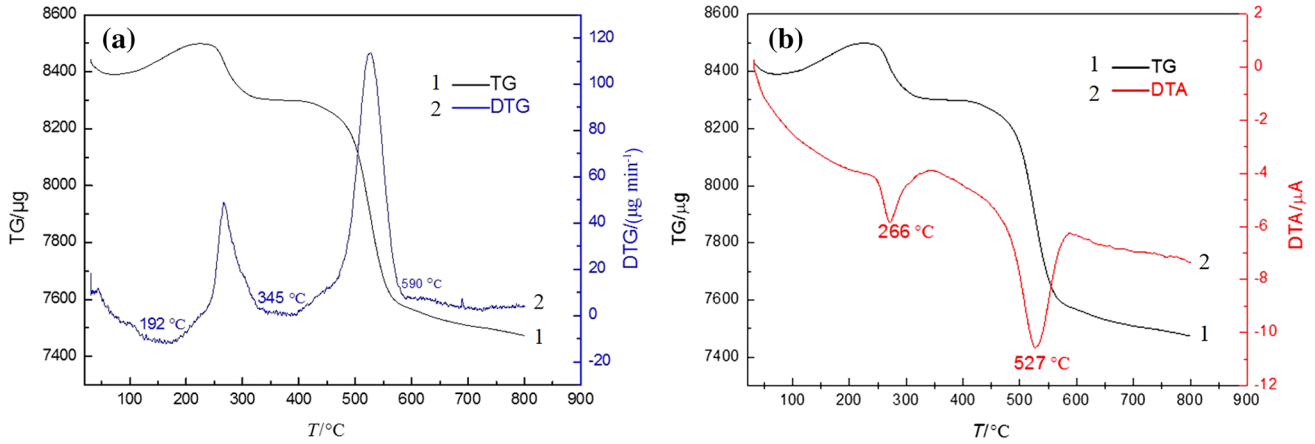

Fig. 13 TG/DTG curve (**a**) and TG–DTA curve (**b**)

$$2FeO(OH)(s) \rightarrow Fe_2O_3(s) + H_2O(g) \quad (8)$$

$$3Fe_2O_3 + H_2 \rightarrow 2Fe_3O_4 + H_2O(g) \quad (9)$$

When the ore was roasted at 400 °C in a hydrogen atmosphere, the free water was firstly vaporized, and part of the diaspore was decomposed to α-Al_2O_3 [Eq. (7)] and the α-Al_2O_3 had low crystallinity due to the low roasting temperature, which should be beneficial for the dissolution properties. On the other hand, the goethite was decomposed to hematite [Eq. (8)] at 200–325 °C, and in this process, numerous micropores were generated due to the dehydration of crystalline. The micropores can contribute to the hematite reduction in hydrogen gas, and thus, all goethite have been reduced to magnetite and hematite [Eqs. (8) and (9)].

4 Conclusion

The advisable dissolution and magnetic separation conditions are given for alumina and iron recovery. For leaching process, the dissolution time is 50 min, dissolution temperature is 260 °C, lime addition amount is 6%, and the Na_2O concentration is 235 g/L, where the alumina dissolution ratio is 79.60%, and the Fe_2O_3 content in red mud is 32.13%. In the magnetic separation, the magnetic separation current is better to be set as 4 A with a magnetic separation time of 10 min for one separation cycle. Under this separation condition, the iron recovery ratio is 56.59% and the Fe_2O_3 content of iron concentrate is 43.46%. Comparing the three recovery processes, the magnetic roasting → magnetic separation → dissolution process shows a better alumina and iron recovery ratio, in which the alumina dissolution ratio is 86.2%, iron recovery ratio is 69.58%, and the Fe_2O_3 content in iron concentrate is 40.66%. The techniques to avoid alumina loss during the magnetic separation and the methods to improve the grade of iron concentrate need more special investigation in the further studies.

Acknowledgements The authors are appreciated for the financial support of the National Natural Science Foundation of China (51574095, 51664005 and 51774102), Guizhou Alumina Production Technology and Technology Science and Technology Innovation Talent Team Project (Qian Ke He Talent Team Giant [2015]0.4005, Qian Ke He Platform Talent [2017]5788 and the Cooperation Talent Group of Guizhou Department [2017]5626), Guizhou Metallurgical Resources Comprehensive Utilization Engineering Research Center Project (Qian Jiao He [2015]334) and Guizhou University Postgraduate Innovation Fund (Research Institute of Technology 2016018).

References

[1] D. Zinoveev, P. Grudinsky, V. Korneev, V. Dyubanov, M. Zheleznyi, Key Eng. Mater. 743 (2017) 331–337.
[2] Z.B. Liu, H.X. Li, Hydrometallurgy 155 (2015) 29–43.
[3] S.G. Xue, F. Zhu, X.F. Kong, C. Wu, L. Huang, N. Huang, W. Hartley, Environ. Sci. Pollut. Res. 23 (2016) 1120–1132.
[4] J.S. Deng, S.M. Wen, S.J. Bai, M.F. Xie, H.Y. Shen, Adv. Mater. Res. 524-527 (2012) 1115–1123.
[5] B. Mishra, A. Staley, D. Kirkpatrick, Miner. Metall. Process 19 (2002) 87–94.
[6] Y. Liu, R. Naidu, Waste Manage. 34 (2014) 2662–2673.
[7] J.K. Sadangi, S.P. Das, A. Tripathy, S.K. Biswal, Sep. Sci. Technol. 53 (2018) 2186–2191.
[8] J.M. Wang, B. Peng, L.Y. Chai, M. Li, N. Peng, Chin. J. Nonferrous Met. 22 (2012) 1455–1461.
[9] C.R. Borra, Y. Pontikes, K. Binnemans, T.V. Gerven, Miner. Eng. 76 (2015) 20–27.
[10] G.H. Li, J. Luo, T. Jiang, Z.X. Li, Z.W. Peng, Y.B. Zhang, Metals 6 (2016) 294.
[11] P. Plescia, D. Maccari, JOM 48 (1996) 25–28.
[12] X.B. Li, Y.L. Wang, Q.S. Zhou, T.G. Qi, G.H. Liu, Z.H. Peng, H.Y. Wang, Trans. Nonferrous Met. Soc. China 27 (2017) 2715–2726.

[13] Z.G. Liu, M.S. Chu, Z. Wang, W. Zhao, J. Tang, High Temp. Mater. Processes 36 (2017) 79–88.
[14] X.L. Hu, W.M. Chen, Q.L. Xie, Trans. Nonferrous Met. Soc. China 21 (2011) 1641–1647.
[15] W. Liu, J. Yang, B. Xiao, J. Hazard. Mater. 161 (2009) 474–478.
[16] Q. Zheng, X. Bian, W.Y. Wu, J. Iron Steel Res. Int. 24 (2017) 147–155.
[17] J.V. Khaki, H. Shalchian, A. Rafsanjani-Abbasi, N. Alavifard, Thermochim. Acta 662 (2018) 47–54.
[18] Y. Man, J. Feng, Powder Technol. 301 (2016) 674–678.
[19] Y.Y. Zhang, W. Lü, Y.H. Qi, Z.S. Zou, Int. J. Miner. Metall. Mater. 23 (2016) 881–890.
[20] G. Li, F. Gu, T. Jiang, J. Luo, B. Deng, Z. Peng, JOM 69 (2017) 315-322.
[21] D.Q. Zhu, T.J. Chun, P. Jian, Z. He, J. Iron Steel Res. Int. 19 (2012) No. 8, 1–5.
[22] M. Samouhos, M. Taxiarchou, G. Pilatos, P.E. Tsakiridis, E. Devlin, M. Pissas, Miner. Eng. 105 (2017) 36–43.
[23] Y.R. Li, J. Wang, X.J. Wang, B.Q. Wang, Z.K. Luan, Phys. C 471 (2011) 91–96.
[24] X.B. Li, F. Niu, G.H. Liu, T.G. Qi, Q.S. Zhou, Z.H. Peng, Trans. Nonferrous Met. Soc. China 27 (2017) 908–916.
[25] P. Basu, in: Essential readings in light metals, Springer, 2016, pp. 176–183.
[26] X.B. Li, S.W. Yu, W.B. Dong, Y.K. Chen, Q.S. Zhou, T.G. Qi, G.H. Liu, Z.H. Peng, Y.Y. Jiang, Hydrometallurgy 152 (2015) 183–189.
[27] X.B. Li, Y.L. Wang, Q.S. Zhou, T.G. Qi, G.H. Liu, Z.H. Peng, H.Y. Wang, Hydrometallurgy 175 (2018) 257–265.
[28] L.Y. Li, Waste Manage. 21 (2001) 525–534.
[29] E. Bujdosó, M. Miskei, J. Radioanal. Chem. 11 (1972) 99–104.
[30] P. Smith, Hydrometallurgy 170 (2017) 16–23.
[31] Y.P. Lan, Q.C. Liu, F. Meng, D.L. Niu, H. Zhao, J. Iron Steel Res. Int. 24 (2017) 165–170.